Wall turbulence with arbitrary mean velocity profiles

By J. Jiménez†

1. Motivation

The original motivation for this work was an attempt to shorten the inflow length that has to be discarded from simulations of zero-pressure-gradient boundary layers. That length had been established by Simens *et al.* (2009) to be a low multiple of the distance by which eddies are advected during a turnover time, $U_\infty \delta_{99}/u_\tau$, where U_∞ is the free-stream velocity, u_τ the friction velocity, and δ_{99} the 99% boundary layer thickness. For moderate Reynolds numbers, the turnover distance is roughly 20–30δ_{99}, which is usually a non-negligible fraction of the simulation box. Since the slowest convergence is for the largest structures, and in particular for the mean velocity profile, it was decided to keep that profile artificially fixed to some theoretical approximation for an initial segment of the layer, including a growth law, with the idea of giving the fluctuations enough fetch in a 'correct' environment before the flow was fully released. The chosen family of profiles was the one developed by Nagib *et al.* (2006) for high-Reynolds-number boundary layers, even if the Reynolds number of our simulation was only moderate, $Re_\theta = 2000$–6000.

The experiment was not successful. The immediate result was the growth of all the Reynolds stresses above their 'natural' values by factors of the order of two. Although they returned to their correct levels once the mean profile was allowed to evolve naturally, the procedure did not shorten the inflow length, and was eventually abandoned. Anecdotal conversations with P. Moin revealed that he had observed a similar effect while testing a related technique to initialize early LES channels, although the details had never been documented, and the method was also abandoned. In the channels, the growth of the fluctuations saturated after a while, but in the boundary layers, which develop spatially from an inflow, it was impossible to determine within a reasonable expenditure of computer time whether that was also the case, or whether the unnatural growth of the fluctuations would continue forever.

Although the technique had not proved successful in either case as a way of decreasing the initial simulation transient, the reasons why the Reynolds stresses grew when the profile was kept fixed remain interesting and unclear. They are the subject of this report. The two obvious alternatives are that the growth of the fluctuations is connected with keeping the mean profile fixed, instead of letting it evolve according to its own equation of motion, or that the fluctuations are sensitive to relatively small deviations of the profile from its 'correct' shape, and that the profiles used in the two cases mentioned above were slightly incorrect.

Both results would be interesting. One of the central problems of wall-bounded turbulence is how structures of different sizes, associated with different wall distances, adjust their relative intensities to balance the mean momentum transfer along the wall-normal direction. It is not difficult to construct conceptual feed-back models in which locally

† School of Aeronautics, Universidad Politécnica, 28040 Madrid, Spain

Case	κ	A	h^+	$10^3 P_{nom}$	$10^3 P_{true}$	Symbol	Profile
C0			549	1.48	1.48	———	From eqs. of motion
C1	0.3	6	559	1.98	3.87	—·—	(2.1)
C2	0.35	14.5	552	1.72	2.43	- - - -	(2.1)
C3	≈ 0.4	≈ 23	546	1.48	1.45	—▽—	Fixed from DNS
C4	0.45	31.5	541	1.47	1.78	—○—	(2.1)
C5	0.5	40	537	1.40	1.70	—△—	(2.1)

TABLE 1. Simulation parameters. All cases are in a computational box $(L_x, L_z) = (\pi h, \pi h/2)$. In all of them, except C0, the mean profile is kept fixed. The parameters κ and A are used in the profile formula (2.1).

weak structures, with insufficient Reynolds stresses, result in the local acceleration of the mean velocity profile, which in turn leads to the enhancement of the velocity gradient and to the strengthening of the local fluctuations. It is conceivable that the effect of fixing the mean profile could be to disturb that feed-back mechanism, which would be the reason for the unnatural fluctuation intensities. But one should beware of two-scale models of turbulence, which in this case would be the scale of the fluctuations and the mean flow. Everything we know about turbulent flows points to their multiscale character, and it is more likely that any interaction leading to the adjustment of the fluctuation intensities at different wall distances takes place between structures of roughly similar sizes, without necessarily passing through the mean flow.

The second alternative is that satisfying the momentum balance is associated with having the correct mean velocity profile, which would in that way be shown to be very special. The classical theory for the mean profile, as represented, for example, by the logarithmic-layer argument of Townsend (1976), is that the turbulent energy production, which is determined by the mean shear and by the transverse Reynolds stress, should balance the dissipation, which is proportional to the (cube of) the fluctuation intensities. This would explain why changing the mean profile, and therefore the production, modifies the intensities, and would imply that the latter are determined locally by the mean shear. It would also suggest an interesting lack of interaction among structures at different wall distances. If that were the case, it would be important to ascertain to what extent the equilibrium relations remain true for profiles different from the canonical one.

This report explores those issues by means of numerical experiments in turbulent channels in which the mean profiles are systematically varied. The next three sections describe, respectively, the numerical experiments, the results, and some preliminary conclusions.

2. Numerical experiments

We denote by x, y and z the streamwise, wall-normal and spanwise coordinate directions, and by u, v and w the corresponding velocity components. Capital letters represent mean values, and primed quantities are root-mean-squared fluctuation intensities. The '+' superscript refers to quantities normalized with the friction velocity and with the kinematic viscosity ν. The brackets $\langle\rangle$ denote averaging over wall-parallel planes and time.

The parameters of the numerical experiments are summarized in Table 1. They are performed in doubly-periodic channels of half-width h, and streamwise and spanwise periodicities πh and $\pi h/2$, respectively. The relatively small boxes result in a slow con-

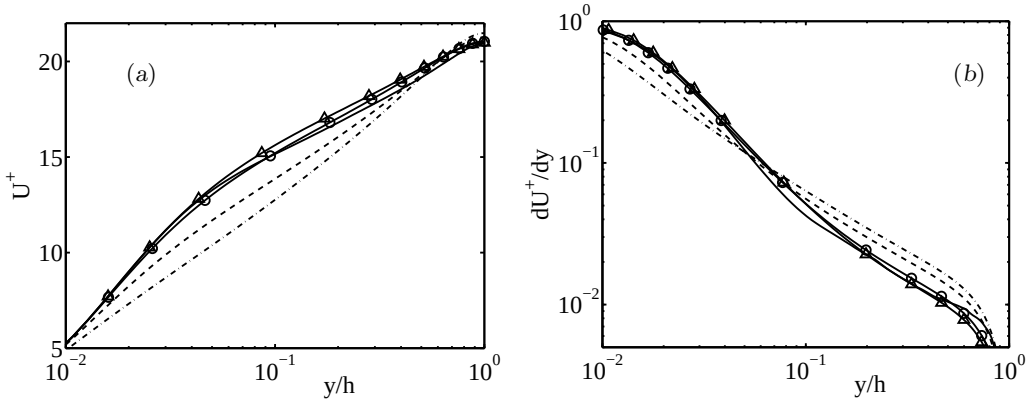

FIGURE 1. (a) Mean velocity of the channel simulations. (*b*) Mean shear. Symbols as in Table 1.

vergence of the statistics, some of which are not very smooth, but they make it more likely that any feedback effect would be visible. For this preliminary survey, the Reynolds number is $h^+ \approx 550$. The numerical code is as in del Álamo & Jiménez (2003), with the mass flux kept constant. The statistics for each case were accumulated for about 15 eddy turnovers, h/u_τ, after discarding initial transients of approximately five turnovers.

Besides the reference case C0, which solves the full Navier–Stokes equations, the rest of the cases substitute the evolution equation of the instantaneous x–z plane averages of the velocities, $u_{00}(y,t)$ and $w_{00}(y,t)$, by fixed profiles $U(y)$ and $W(y) = 0$. Continuity implies that $v_{00}(y,t) = 0$. The simplest case is C3, where $U(y)$ is made to coincide with the long-term averaged velocity profile of the large-box channel simulation in del Álamo & Jiménez (2003), which is assumed to be 'correct'.

The rest of the experiments use a fixed velocity profile derived from the Cess (1958) approximate formula for total (molecular plus eddy) viscosity,

$$\frac{\nu_{tot}}{\nu} = \frac{1}{2}\left\{1 + \frac{\kappa^2 {h^+}^2}{9}\left[2Y - Y^2\right]^2\left[3 - 4Y + 2Y^2\right]^2\left[1 - \exp\left(\frac{-Yh^+}{A}\right)\right]^2\right\}^{1/2} + \frac{1}{2}, \tag{2.1}$$

where $Y = y/h$. The mean velocity is obtained from Eq. (2.1) by integrating the momentum equation $\partial_y U = u_\tau^2(1-Y)/\nu_{tot}$.

The two parameters κ and A are roughly equivalent to the Kármán constant and to the square of the intercept of the logarithmic velocity profile. The 'natural' profile for $h^+ = 550$ is approximated well by $\kappa = 0.4$ and $A = 23$, which were used to rerun case C3, with results that were indistinguishable from those using the DNS profile. Other cases were chosen to yield the same mass flux and friction Reynolds number. To keep some consistency among the cases, an attempt was made to maintain the same total production for all the cases,

$$P_{true} = U_b^{-3}\int_0^h -\langle uv\rangle \partial_y U \,\mathrm{d}y. \tag{2.2}$$

Unfortunately, the Reynolds stress is not known beforehand, because, as we will see below, the channels are not in equilibrium, and the stress can only be estimated by assuming that the total stress, $\tau_{xy} = -\langle uv\rangle + \nu\partial_y U$, is equal to $u_\tau^2(1-y/h)$, as in the

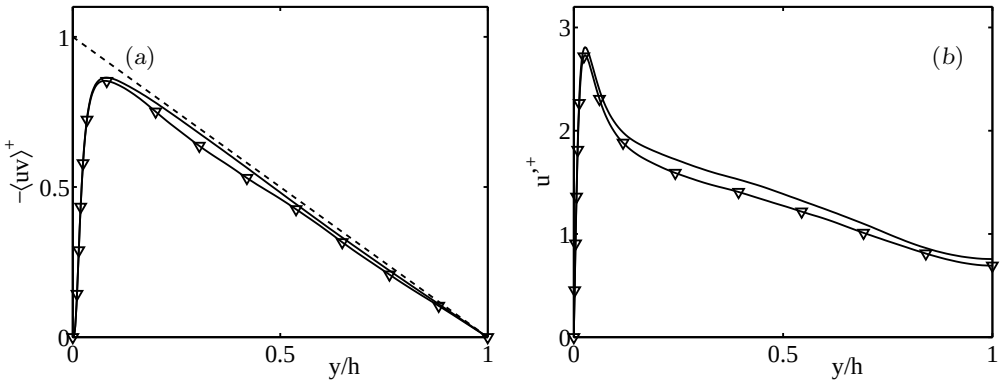

FIGURE 2. Effect on the fluctuations of fixing the mean velocity profile to the 'correct' one obtained from an independent DNS (cases C0 and C3). (a) Reynolds stress $-\langle uv \rangle$. (b) Streamwise velocity fluctuations. Symbols as in Table 1.

natural case. The result is a 'nominal' production,

$$P_{nom} = U_b^{-3} \int_0^h \left[u_\tau^2 (1 - y/h) - \nu \partial_y U \right] \partial_y U \, \mathrm{d}y, \tag{2.3}$$

which was kept approximately constant among cases. The resulting empirical relation, $A = 170\kappa - 45$, is satisfied for all the cases in Table 1. In practice, because of various inconsistencies between the way the simulation was implemented and the definition of the profiles, both Re_τ and P_{nom} varied somewhat among cases, although less than P_{true}. Their actual values are given in able 1. The resulting profiles, together with their corresponding mean velocity gradients, are given in figures 1(a) and 1(b), which show that the effect of increasing κ is to flatten the profile, and to move the gradient towards the wall.

3. Results

Figure 2 shows the result of fixing the profile to the 'correct' value from the simulation of del Álamo & Jiménez (2003). The differences with the reference case C0 are minor, and the two flows can be considered identical within statistical uncertainty. This suggests that the problems observed in the boundary-layer simulations were due not to fixing the mean velocity, but to the choice of incorrect profiles, and that the feedback mechanism mentioned in the introduction is either inactive at the scale of the mean velocity, or inhibited by the use of the correct profile.

On the other hand, imposing a profile different from the natural one has a major effect on the fluctuations. Figure 3(a) shows that more rounded profiles, corresponding to lower κ and to higher velocity gradients away from the wall, have much stronger Reynolds shear stresses than the natural case. Conversely, flatter profiles have somewhat higher stresses near the wall, and lower ones away from it, although the effect is weaker. Those changes are not only due to the need to compensate for the modified viscous stress created by the new velocity gradient. Figure 3(b) shows that the differences persist for the total stress, τ_{xy}^+, which would be $(1-Y)$ if it only had to balance a uniform pressure gradient. In fact, fixing the profile is equivalent to adding to the flow a volume force, and the right-hand side of the total momentum equation can no longer be assumed to be uniform. Figure 3(b) shows that the 'rounded' profiles with the lower κ are subject to a strong accelerating

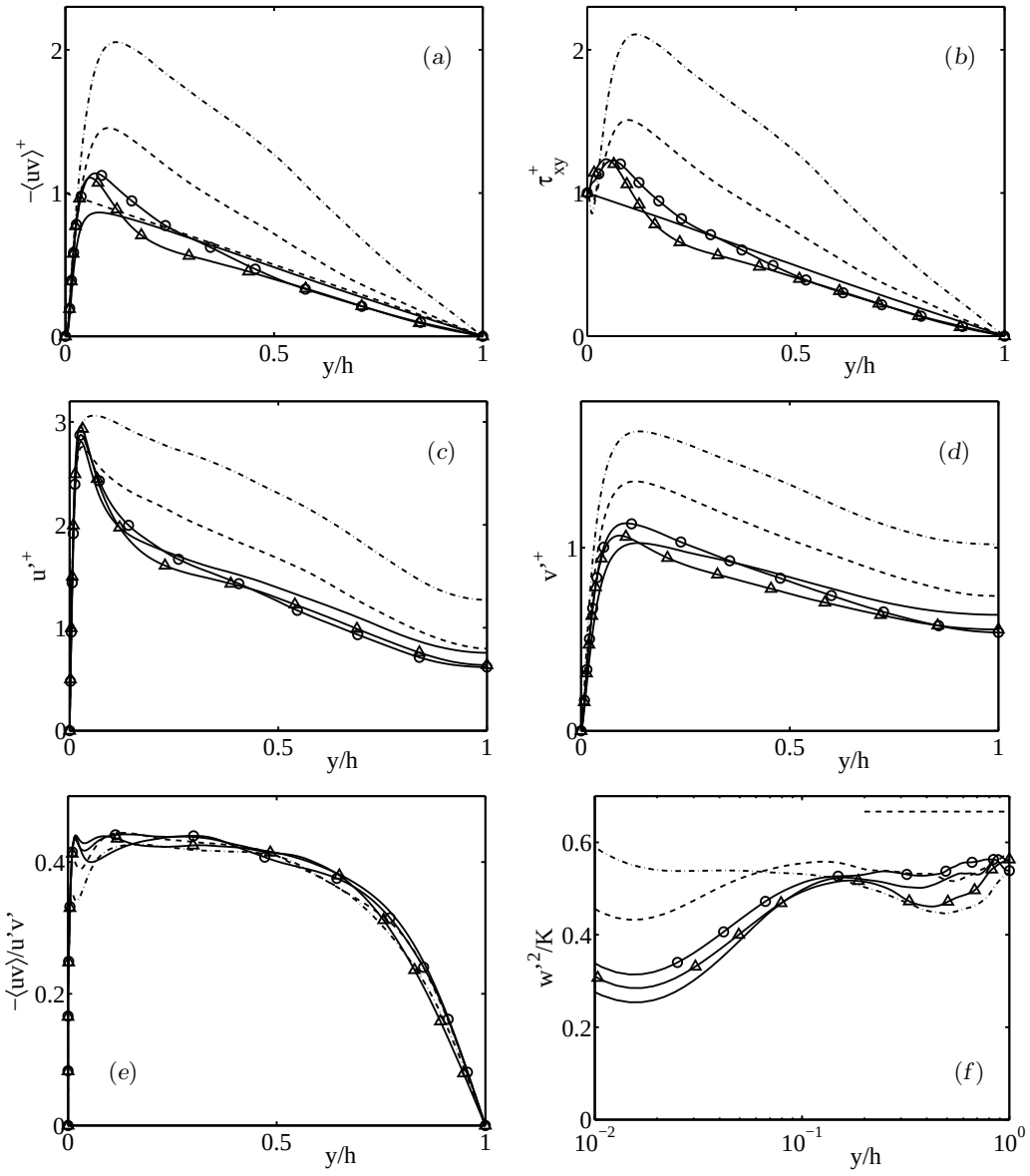

FIGURE 3. Distribution of: (*a*) the Reynolds stress $-\langle uv\rangle$. (*b*) Total stress $-\langle uv\rangle + \nu\partial_y U$. (*c*) Intensity of the streamwise velocity fluctuations, and (*d*) of the wall-normal velocity fluctuations. (*e*) Structure coefficient $-\langle uv\rangle/(u'v')$. (*f*) Spanwise energy fraction w'^2/K. The dashed horizontal line in (*f*) corresponds to isotropy. Symbols as in Table 1.

force trying to adjust the mean profile to its natural value, and that the same is true near the wall for the flatter profiles. The diagonal Reynolds stresses also change. Figures 3(*c*) and 3(*d*) show the intensities of the streamwise and wall-normal velocity fluctuations, both of which follow trends similar to those of the transverse stress.

Other flow properties are less affected. For example, although not shown here, the production and dissipation always remain in approximate local equilibrium away from the wall and from the center of the channel, and the integral length, defined as $K^{3/2}/\epsilon$,

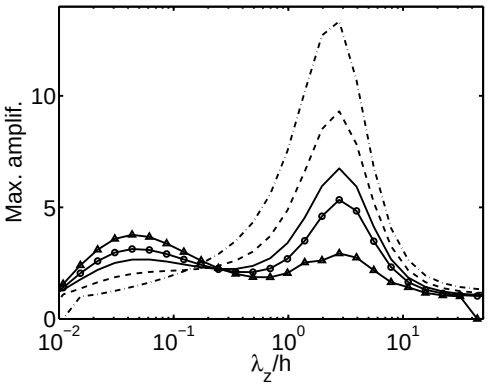

FIGURE 4. Maximum linear transient amplification of perturbations with streamwise wavelength $\lambda_x = 10h$, as a function of the spanwise wavelength λ_z. Channels with $h^+ = 2000$, and profiles defined with the parameters κ and A in Table 1.

where K is the turbulent kinetic energy and ϵ the dissipation, increases approximately linearly with the wall distance below $y \approx 0.4h$, in what could be interpreted as an approximate logarithmic layer.

Figures 3(e) and 3(f) show two measures of the isotropy of the velocity fluctuations. Figure 3(e) shows the structure coefficient of the transverse Reynolds stress, $-\langle uv\rangle/(u'v')$, which varies little with respect to the natural channel, suggesting that the fluctuations created by the non-standard profiles are essentially similar to the natural ones, although stronger or weaker depending on the case. The exception is the behavior near the wall, where the structure coefficient drops for the cases with the more rounded profiles, presumably because their stronger fluctuations extend to the wall as at least partially inactive motions that do not create shear stresses. The main 'inactive' component turns out to be the spanwise one. Figure 3(f) displays the isotropy coefficient $I_w = w'^2/K$, which varies from $I_w = 2$ for purely spanwise motions, to $I_w = 0$ for velocities entirely contained within the x–y plane, to $I_w = 2/3$ for isotropic flows. The main difference among the different cases is that the fraction of the energy due to w' increases with decreasing κ below $y^+ \approx 50$. Somewhat surprisingly, the other velocity component whose relative importance increases in that region is the wall-normal one v', suggesting that the new structures are predominantly contained in the cross-stream plane. Note that this could conceivably be a consequence of the small simulation boxes.

3.1. *Linear stability*

It is interesting that the qualitative features of the changes in the fluctuation intensities can be correlated with the maximum linear amplification that perturbations can undergo. Figure 4 shows the maximum amplifications of long structures ($\lambda_x/h \approx 10$) in channels, given as functions of the spanwise wavelength for the same combinations of κ and A as in Table 1. They are obtained using the method of del Álamo & Jiménez (2006), with the eddy viscosity in Eq. (2.1). As in that paper, the amplification has two peaks. The first one, at $\lambda_z \approx 2h$, corresponds to eigenfunctions associated with the central part of the channel, while the second one, at $\lambda_x^+ \approx 100$, represents narrow structures concentrated in the sublayer. Note that the Reynolds number for this analysis has been increased to $h^+ = 2000$ to provide a clearer separation between the inner and outer scales.

What is interesting is that the rounded profiles with low κ, for which the shear has

moved away from the wall, amplify more strongly the outer structures, and only weakly the sublayer ones, and that the opposite is true for the flatter profiles. That behavior is strongly reminiscent of the intensity changes discussed in the previous section, and supports the hypothesis that the magnitude of the fluctuations is determined by the local mean shear, rather than by interactions with structures at other wall distances. The exception is the 'attached' nature of the outer eddies, whose influence extends to the wall, as discussed in the previous section.

4. Conclusions and future work

While a lot more work is needed to fully understand the results presented in this report, they suggest that the mechanism that controls the mean velocity profile in wall-bounded turbulent flows is relatively simple. The local velocity gradient determines the energy that flows into fluctuations at a given wall distance, which grow until they activate an energy transfer strong enough to balance the production. Those fluctuations are essentially 'natural', although of variable amplitude, and therefore carry transverse Reynolds stresses that, in turn, determine the mean profile. As mentioned in the introduction, that mechanism is unlikely to work only on the mean velocity, and it is probably also active between fluctuations of sufficiently different sizes, which would control each other.

The modification of the fluctuation intensities by the distorted profiles is consistent with the maximum relative linear amplification of perturbations with eigenfunctions associated with the different wall distances, and it is interesting that the profiles observed in natural flows are those for which the amplification is approximately the same for the inner and outer eigenfunctions. It is difficult not to recall in that context the early suggestion by Malkus (1956) that the mean velocity profile is determined by its marginal linear stability with respect to arbitrary perturbations, although it would now have to be understood in the sense of transient amplification, rather than of exponential instability.

Another interesting aspect of the present results is that they provide a mechanism for controlling turbulence above the buffer layer, at least numerically, which, although probably difficult to implement in real flows, could be used as a tool to study the cause-effect relationships in wall turbulence. They also suggest that the usefulness of artificially fixing the mean velocity profile as a means of accelerating the initial convergence of turbulence simulations should be revisited, although care should be exercised in the choice of the imposed profiles.

Acknowledgments

This work was supported in part by the CICYT grant TRA2009-11498, and by the Advanced Simulation and Computing program of the Department of Energy. I am grateful to Oscar Flores and Florian Tuerke for their careful critique of an early version of this manuscript.

REFERENCES

del Álamo, J. C. & Jiménez, J. 2003 Spectra of very large anisotropic scales in turbulent channels. *Phys. Fluids* **15**, L41–L44.

del Álamo, J. C. & Jiménez, J. 2006 Linear energy amplification in turbulent channels. *J. Fluid Mech.* **559**, 205–213.

Cess, R. D. 1958 A survey of the literature on heat transfer in turbulent tube flow. Report 8-0529-R24. Westinghouse Research.

Malkus, W. V. R. 1956 Outline of a theory of turbulent shear flow. *J. Fluid Mech.* **1**, 521 – 539.

Nagib, H. M., Chauhan, K. A. & Monkewitz, P. 2006 Approach to an asymptotic state for zero pressure gradient turbulent boundary layers. *Phil. Trans. R. Soc. London, Ser. A* **365**, 755–770.

Simens, M., Jiménez, J., Hoyas, S. & Mizuno, Y. 2009 A high-resolution code for turbulent boundary layers. *J. Comput. Phys.* **228**, 4218–4231.

Townsend, A. A. 1976 *The structure of turbulent shear flow*, 2nd edn. Cambridge U. Press.